Received: 10 July 2019 | Revised: 23 September 2019 | Accepted: 6 November 2019

DOI: 10.1002/jimd.12189

ORIGINAL ARTICLE

JIMD SSIEM WILEY

Pharmacokinetics and distribution of 2-hydroxypropyl-β-cyclodextrin following a single intrathecal dose to cats

Mark L. Kao[1] | Susan Stellar[1] | Eric Solon[2] | Alfred Lordi[3] | Nicole Kasica[4] | Gary Swain[4] | Jessica H. Bagel[4] | Brittney L. Gurda[4] | Charles H. Vite[4]

[1]Janssen Research & Development, LLC, Raritan, New Jersey

[2]Madrigal Pharmaceuticals, West Conshohocken, Pennsylvania

[3]XenoBiotic Laboratories, Inc, Plainsboro, New Jersey

[4]Department of Clinical Sciences and Advanced Medicine, School of Veterinary Medicine, University of Pennsylvania, Philadelphia, Pennsylvania

Correspondence
Mark L. Kao, Janssen Research & Development, LLC, 1000 Route 202 South, Raritan, NJ 08869.
Email: mkao@its.jnj.com

Communicating Editor: Markus Ries

Funding information
Ara Parseghian Medical Research Foundation, Grant/Award Number: na; Dana's Angels Research Trust, Grant/Award Number: n/a; German Research Foundation, Grant/Award Numbers: R01-HD045561, R01 NS053677; Janssen Research and Development, Grant/Award Number: NA; National Institutes of Health, Grant/Award Numbers: R01-NS073661, P40-02512; National Niemann-Pick Disease Foundation, Grant/Award Numbers: R01 NS081985, P30 DK020579

Abstract

2-Hydroxypropyl-β-cyclodextrin (HP-β-CD) is an experimental therapy for Niemann-Pick disease type C (NPC) that reduced neuronal cholesterol and ganglioside storage, reduced Purkinje cell death, and increased lifespan in *npc1*−/− mice and NPC1 cats. In this study, tissue distribution was investigated in normal cats that received a single 120-mg dose of [^{14}C]-HP-β-CD (approximately 200 μCi/cat) via the cerebellomedullary cistern (CBMC) and lumbar cistern. One cat was euthanized at each of various time points up to 24 hours postdose for subsequent processing and quantitative whole-body autoradiographic analysis. HP-β-CD-derived radioactivity absorbed from the CBMC was widely distributed to cat tissues; most tissues were observed to have reached their highest concentration at 1 hour postdose. HP-β-CD-derived radioactivity penetrated into the deeper parts of the central nervous system with the highest concentration at 4 hours (403 μg Eq/g or 0.28 mM) and remained high (49.7 μg Eq/g or 0.03 mM) at 24 hours. The relatively long half-life (11-30 hours) in cerebral ventricles and the subarachnoid space surrounding the brain and spinal cord might contribute to the efficacy of HP-β-CD in NPC1 cats. Other tissues with high concentrations of radioactivity were nasal turbinates, pituitary gland, and urinary bladder, while relatively low concentrations were observed in blood and bile.

KEYWORDS

animal model, brain, cholesterol, drug therapy, inborn errors of metabolism, Niemann Pick type C, storage diseases

Abbreviations: AUC, area under the tissue concentration-time curve; AUC_{inf}, AUC from time 0 to infinity with extrapolation of the terminal phase; AUC_{last}, AUC from time 0 to the time correspondent to the last quantifiable concentration; CBMC, cerebellomedullary cistern; C_{max}, maximal observed tissue concentration; CSF, cerebrospinal fluid; ER, endoplasmic reticulum;; HP-β-CD, 2-Hydroxypropyl-β-cyclodextrin; IT, intrathecal; LC, lumbar cistern; LLOQ, lower limit of quantification; NIH, National Institutes of Health; NPC, Niemann-Pick disease type C; QWBA, quantitative whole-body autoradiography; RT, room temperature; $t_{1/2}$, half-life.

1 | INTRODUCTION

Cyclodextrins are cyclic oligosaccharides with hydrophobic interiors used as formulation vehicles to increase the amount of drug, including hormones and vitamins, which can be solubilised in aqueous solutions.[1] 2-Hydroxypropyl-β-cyclodextrin (HP-β-CD) has been extensively studied in rodents, dogs, and monkeys where it is generally well tolerated at low doses.[2]

Niemann-Pick disease type C (NPC) is an incurable lysosomal storage disorder characterised by the endolysosomal accumulation of unesterified cholesterol and sphingolipids, progressive neurological dysfunction, hepatosplenomegaly, and early death.[3,4] NPC results from mutations in either *NPC1* or *NPC2* genes, with the majority of patients having mutations in *NPC1*.[3] Weekly intraperitoneal administration of 1500 mg/kg of HP-β-CD to *npc1−/−* mice resulted in decreased hepatic cholesterol storage and delayed onset of continuous extensor tremors of the limbs.[4] Administration of single or multiple subcutaneous doses of 4000 mg/kg of a 20% solution of HP-β-CD to *npc1−/−* mice reversed the defect in the lysosomal transport of cholesterol and significantly improved hepatic dysfunction, decreased lipid accumulation and neurodegeneration, and prolonged lifespan.[5,6] Subcutaneous administration of 4000 and 8000 mg/kg HP-β-CD to naturally-occurring NPC1 cats also achieved some neurological improvements, however, those receiving 8000 mg/kg developed pulmonary toxicity or injection site intolerability.[7] In contrast, intrathecal (IT) administration of 120-mg HP-β-CD via the cerebellomedullary cistern (CBMC) every 2 weeks to NPC1 cats dramatically reduced neurological dysfunction, lipid accumulation in neurons, Purkinje cell death and extended animal life while avoiding pulmonary toxicity and injection site pain.[7] Clear evidence of the therapeutic potential of IT administration of HP-β-CD in the animal model of NPC disease led to a Phase 1/2a National Institutes of Health (NIH) human clinical trial in 2013 (ClinicalTrials.gov identifier NCT01747135)[8] and a Phase 2b/3 trial that began in 2015 (ClinicalTrials.gov identifier NCT02534844) sponsored by Mallinckrodt Pharmaceuticals (Staines-upon-Thames, United Kingdom). This current study investigates the central nervous system (CNS) distribution of HP-β-CD following administration of [^{14}C]-HP-β-CD to cats via the IT administration route. The possible relationship between target concentration and the efficacy toward NPC disease is discussed.

2 | MATERIALS AND METHODS

2.1 | Chemicals and HP-β-CD formulation

Two lots of [^{14}C]-HP-β-CD labelled at the hydroxylpropyl side chain were used in the study. The first lot, used for the 0.25-, 1-, and 4-hour postdose samples of the cat study, was obtained from Sphingo Biotech Inc. (High Springs, Florida). The [^{14}C]-HP-β-CD, which had a specific activity of 6.95 μCi/mg, was purified and diluted with unlabelled HP-β-CD (Trappsol, Cyclo Therapeutics, Alachua, FL) to yield a specific activity of 1.76 μCi/mg and radiochemical purity of 99.8%. The second lot, used for the 8-, 12-, and 24-hour postdose samples, was obtained from Janssen Research & Development (Beerse, Belgium). This lot of [^{14}C]-HP-β-CD had a specific activity of 1.64 μCi/mg and radiochemical purity of 97.2% (KleptoseHPB, Roquette, Geneva, IL). The molecular weight of the two [^{14}C]-HP-β-CD lots ranged from 1380 to 1480 Da, with an average of approximately 1440 Da. Other chemicals used in this study were of the highest purity commercially available.

2.2 | Animal experiments

Cats were raised in the Referral Center for Animals Models of Human Genetic Disease at the School of Veterinary Medicine, University of Pennsylvania (NIH OD P40-10939), under NIH and US Department of Agriculture guidelines for the care and use of animals in research. All institutional and national guidelines for the care and use of laboratory animals were followed.

A total of 8 normal cats were enrolled in the tissue distribution study.

The study was conducted with [^{14}C]-HP-β-CD administered to the IT space. [^{14}C]-HP-β-CD was dissolved in saline to achieve a concentration of 200 mg/mL. The first distribution experiment involved six cats of either gender that each received a single injection of [^{14}C]-HP-β-CD via the CBMC. In the follow-up study, 1 male and 1 female cat each received a single injection via the lumbar cistern (LC). Cats were anaesthetised with intravenous propofol (up to 6 mg/kg; Abbott Laboratories, Chicago, Illinois). A 20-gauge spinal needle was placed into the CBMC or LC and approximately 1.0 mL of cerebrospinal fluid (CSF) was removed. Immediately following CSF removal, 0.6 mL of 20% [^{14}C]-HP-β-CD in sterile saline was injected over a 2-minute period. In each group, cats received a target dose of 120 mg/cat (approximately 4000 mg/kg for a 30-g brain weight) using a 200 mg/mL sterile solution of [^{14}C]-HP-β-CD. This resulted in a final radioactive dose of approximately 200 μCi/cat. One cat from the CBMC group was euthanized at each of the following time points: 0.25, 1, 4, 8, 12, and 24 hours postdose, and one cat each from the LC group was euthanized at 8 and 12 hours postdose. The euthanized animals were placed in dry ice and the carcasses frozen in hexane dry ice bath for subsequent processing and quantitative whole-body autoradiography (QWBA) analysis.

2.3 | QWBA tissue distribution

The frozen carcasses from each cat were embedded in a 2% carboxymethylcellulose matrix and mounted on a microtome stage (Leica CM3600 Cryomacrocut, Nussloch, Germany) maintained at approximately −20°C. Three quality control standards, which were plasma fortified with [^{14}C]-glucose at approximately 0.05 μCi/g, were placed into each frozen block prior to sectioning and were used for control of section thickness. Sections approximately 40 μm thick were taken in the sagittal plane and captured on adhesive tape (Scotch Tape No. 8210; 3M Ltd., St. Paul, Minnesota). Appropriate sections, selected at various levels of interest in each block, were collected to encompass the following tissues, organs, and biological fluids where possible: adipose (white and brown), adrenal gland, blood (cardiac), bile (in gall bladder), bone, bone marrow, brain (cerebrum, cerebellum, medulla), cecum (and contents), epididymis, eye (uveal tract and lens), kidney (renal cortex and medulla), large intestine (and contents), liver, lung, lymph nodes, myocardium, ovary, pancreas, pituitary gland, prostate, salivary gland, seminal vesicles, skeletal muscle, skin (non-pigmented and pigmented), small intestine (and contents), spinal cord, spleen, stomach (contents and gastric mucosa), testis, thymus, thyroid, uterus, urinary bladder, and its contents.

Tissue sections were allowed to dry by sublimation in the cryomicrotome at −20°C for at least 48 hours. A set of sections was mounted on a cardboard backing, covered with a thin plastic wrap, and exposed along with [^{14}C]-calibration standards ([^{14}C]-glucose mixed with blood at 10 different concentrations at approximately 0.0007 to 7.41 μCi/g) to a [^{14}C]-sensitive phosphor imaging plate [Fuji Biomedical, Stamford, Connecticut]). The imaging plate and sections were placed in light-tight exposure cassettes, in a copper-lined lead safe at room temperature (RT) for a 4-day exposure period. The imaging plates were scanned at 100 μm using the Typhoon 9410 image acquisition system (GE Healthcare/Molecular Dynamics, Sunnyvale, California) and the resultant images stored on a dedicated computer. Quantification was performed by image densitometry using MCID image analysis software (v. 7.0; Interfocus Imaging, Cambridge, United Kingdom), and a standard curve constructed from the integrated response (molecular dynamic count/mm^2) and the nominal concentrations of the [^{14}C]-calibration standards. The concentrations of radioactivity were expressed as μCi/g and were converted to μg equivalents of cyclodextrin per gram sample (μg Eq/g) using the specific activity of administered [^{14}C]-HP-β-CD (1.76 μCi/mg). A lower limit of quantification (LLOQ) was applied to the data. The LLOQ was determined by using the radioactive concentration (μCi/g) of the lowest calibration standard used to generate a calibration curve divided by the specific activity of the test article (1.76 μCi/mg). The upper limit of quantification and LLOQ for QWBA analysis were assessed at 4210.5 and 0.4 μg Eq/g, respectively for data collected on the CBMC cats at 0.25 and 1 hours postdose; at 3282.0 and 0.2 μg Eq/g for the CBMC cats harvested at 4, 8, 12, and 24 hours postdose; and at 4759.6 and 0.6 μg Eq/g for the LC cats at 8 and 12 hours postdose.

2.4 | Filipin staining

In a previous therapeutic study,[7] we injected NPC1 cats with 120 mg HP-β-CD every 2 weeks for life via the CBMC beginning at 3 weeks of age. Three 24-week-old NPC1 cats were evaluated for cholesterol storage in neurons using filipin staining. Fixed-frozen tissue sections were quenched with 1.5 mg/mL glycine for 10 minutes at RT to remove endogenous aldehydes. The sections were washed three times with Phosphate-buffered saline (PBS) (2 minutes each), followed by permeabilisation with 0.02% saponin (Sigma-Aldrich [#S7900]), and then washed three times in PBS (2 minutes each) at RT. Sections were then incubated in a 0.05 mg/mL filipin (Sigma-Aldrich, St Louis, Missouri) solution for 2 hours, in the dark, at RT. Sections were then washed with PBS as previously described and mounted with KPL fluorescent mounting media (SeraCare, Milford, Massachusetts). Sections were viewed for filipin stain with a ultraviolet filter on an epifluorescent microscope.

Cats were raised in the Referral Center for Animals Models of Human Genetic Disease at the School of Veterinary Medicine, University of Pennsylvania (NIH OD P40-10939), under NIH and US Department of Agriculture guidelines for the care and use of animals in research.

3 | RESULTS

Central nervous system tissue concentration of [^{14}C]-HP-β-CD following CBMC administration to normal cats reveals widespread distribution. Whole-body autoradiography was used to visually assess the overall tissue distribution as a function of time. At 0.25 and 1 hours postdose, radioactivity was evident in the subarachnoid space and in the brain and spinal cord parenchyma immediately adjacent to the subarachnoid space (Supplemental Figures S1 and S2). By 4 hours postdose, a concentration gradient of distribution was visible in the brain parenchyma with the darkest regions adjacent to the subarachnoid space and the lightest regions farthest from the subarachnoid space (Supplemental Figure S3) (Figures 1–3).

At 0.25 hours postdose, most of the radioactivity was observed in CSF, where the concentration was determined to be 4194.7 μg Eq/g in the subarachnoid space at the level of the high cervical spinal cord and 4026.6 μg Eq/g in the fourth ventricle (Table 1). In contrast, the concentration in the subarachnoid space at the level of the cerebral cortex was only 11.3 μg Eq/g, and the concentration in the lateral cerebral ventricle was 5.4 μg Eq/g. Penetration into the

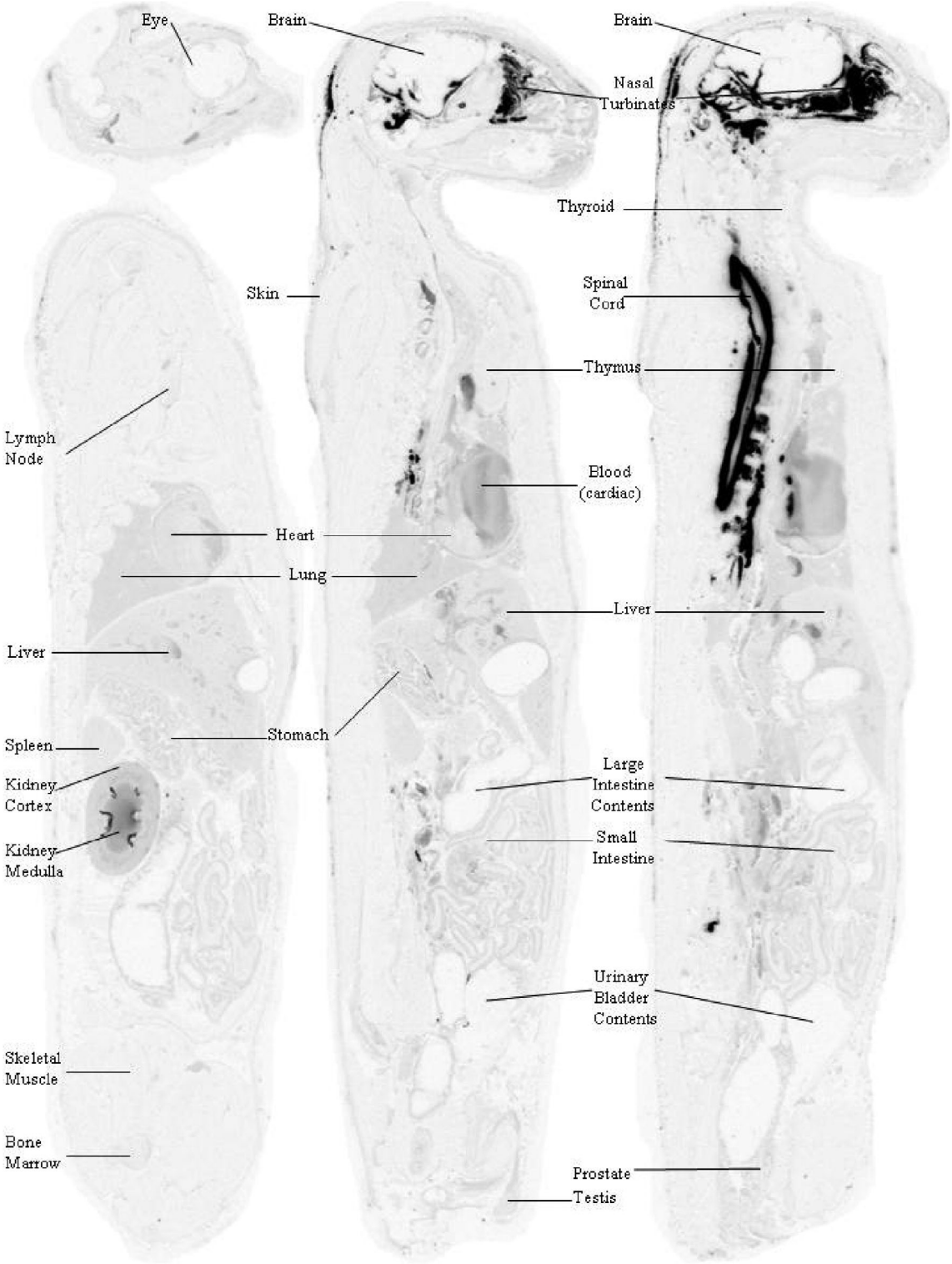

FIGURE 1 Whole-body autoradiogram of the radioactivity distribution in a normal cat at 0.25 hours postdose, following a single 120-mg intrathecal injection of [^{14}C]-HP-β-CD at the CBMC. Sections are parasagittal and sagittal. CBMC, cerebellomedullary cistern; HP-β-CD, 2-hydroxypropyl-β-cyclodextrin

brain at 0.25 hours postdose was limited to regions immediately adjacent to the subarachnoid space (Table 1; Supplemental Figure S1) where concentrations were relatively low (ranging from 1.4 μg Eq/g in the frontal lobe to 23.6 μg Eq/g in the cerebellum). The highest concentration in CNS tissue at this time point was in the cervical spinal cord (278.4 μg Eq/g) immediately adjacent to the cerebellomedullary cistern. Interestingly,

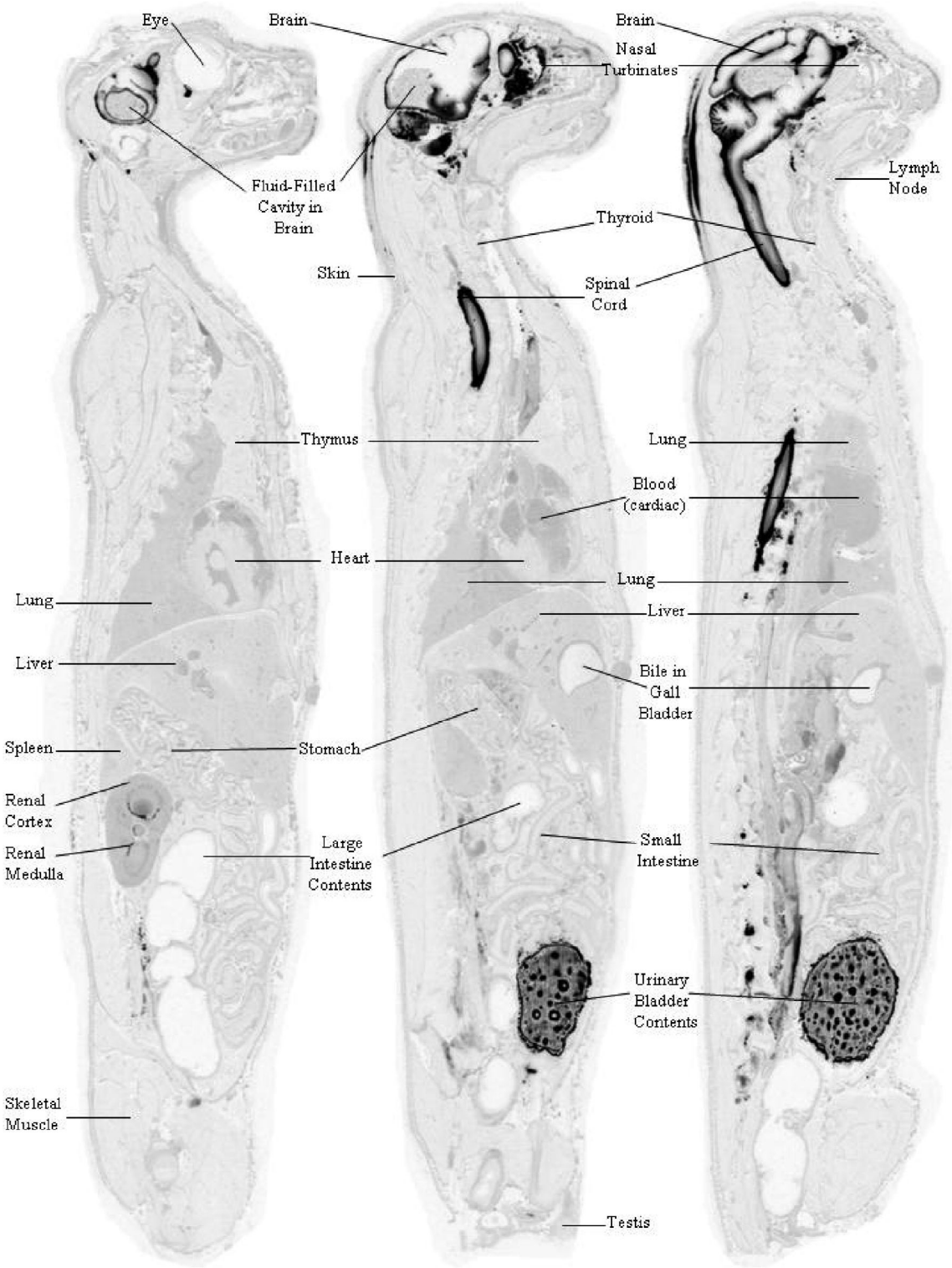

FIGURE 2 Whole-body autoradiogram of the radioactivity distribution in a normal cat at 1 hour postdose, following a single 120-mg intrathecal injection of [^{14}C]-HP-β-CD at the CBMC. Sections are parasagittal and sagittal. CBMC, cerebellomedullary cistern; HP-β-CD, 2-hydroxypropyl-β-cyclodextrin

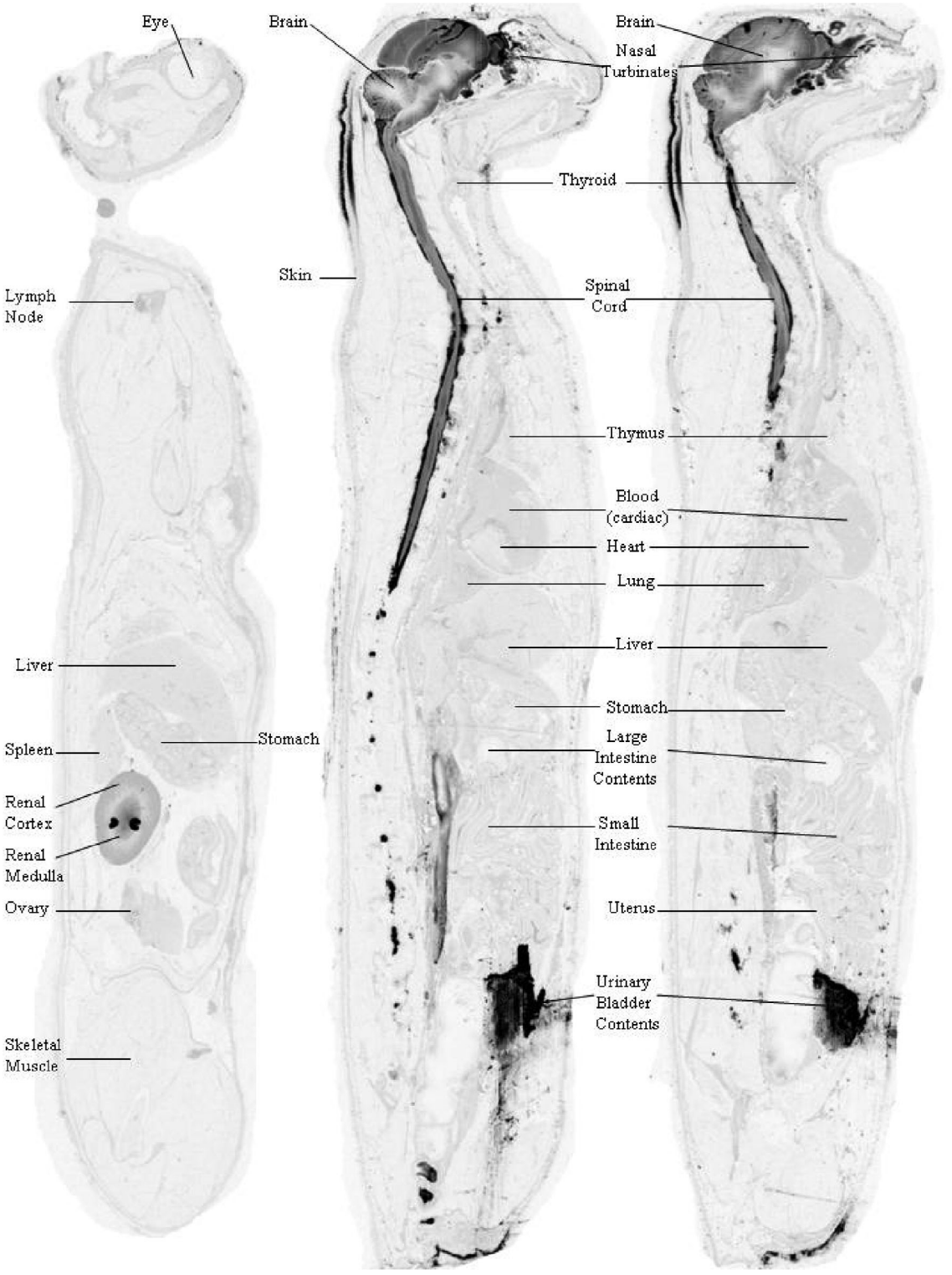

FIGURE 3 Whole-body autoradiogram of the radioactivity distribution in a normal cat at 4 hours postdose, following a single 120-mg intrathecal injection of [^{14}C]-HP-β-CD at the CBMC. Sections are parasagittal and sagittal. CBMC, cerebellomedullary cistern; HP-β-CD, 2-hydroxypropyl-β-cyclodextrin

the highest extraneural tissue concentration observed during the study occurred at this time point in the nasal turbinates (1031.5 μg Eq/g; Table 1). This may have been a result of the highly developed and close association of the olfactory nervous system with the brain and subarachnoid space. The highly vascularized nasal turbinates may have functioned as a site of exchange of the test article from the CSF into the blood vascular system.

TABLE 1 Concentration profile of total radioactivity in regions of the CNS of normal cats after a single 120-mg intrathecal injection of [^{14}C]-HP-β-CD at the CBMC

	CNS [^{14}C]-HP-β-CD Concentration (μg Eq/g tissue)					
Tissue	**0.25 h[a]**	**1 h[a]**	**4 h[a]**	**8 h[b]**	**12 h[b]**	**24 h[b]**
Blood (cardiac)	37.1	40.0	9.2	0.8	0.4	1.3
Nasal turbinates	1031.5	528.1	223.7	55.1	58.4	31.2
Dorsal cerebral cortex, frontal lobe	BQL	1.2	204.6	84.4	70.5	40.6
Ventral cerebral cortex, frontal lobe	1.4	107.4	188.0	92.8	61.4	40.5
Dorsal cerebral cortex, parietal lobe	BQL	3.6	188.4	87.5	74.4	44.1
Ventral cerebral cortex, temporal lobe	BQL	187.9	59.0	26.0	42.7	18.5
Dorsal midbrain	2.9	1.2	166.1	101.5	34.2	20.1
Ventral midbrain	0.7	229.5	61.8	24.8	36.2	15.5
Dorsal cerebellum	2.4	275.1	65.3	83.2	34.9	27.0
Ventral cerebellum	23.6	263.9	195.9	87.0	40.1	18.0
Dorsal medulla	3.9	28.1	21.7	9.0	20.2	18.9
Ventral medulla	7.3	167.9	137.9	28.4	33.1	12.6
Dorsal cervical spinal cord	259.7	302.5	113.4	28.2	24.8	7.2
Ventral cervical spinal cord	278.4	221.3	101.4	19.5	34.5	11.9
Cerebral ventricle (lateral)	5.4	1615.0	79.9	31.0	38.6	17.1
Cerebral ventricle (fourth)	4026.6	3173.9	84.3	59.0	3.3	22.4
Subarachnoid space (high cervical spinal cord)	4194.7	3629.8	59.4	52.4	49.5	36.6
Subarachnoid space (cerebral cortex)	11.3	1054.4	1726.5	226.0	152.6	85.0

Note: The lower limit of quantification was determined by using the radioactive concentration (μCi/g) of the lowest calibration standard used to generate a calibration curve divided by the specific activity of the test article (1.76 μCi/mg).

Abbreviations: BQL, below quantification limit; CBMC, cerebromedullary cistern; CNS, central nervous system; HP-β-CD, 2-hydroxypropyl-β-cyclodextrin.

[a]Specific activity of [^{14}C]-HP-β-CD 1.76 μCi/mg and radiochemical purity of 99.8%.

[b]Specific activity of [^{14}C]-HP-β-CD 1.64 μCi/mg and radiochemical purity of 97.2%.

The blood concentration at 0.25 hours postdose was determined to be 37.1 μg Eq/g.

At 1 hour postdose, many CNS parenchymal regions were observed to have reached their highest concentration (7 of 12 evaluated; Table 1) presumably due to the continued high concentration of [^{14}C]-HP-β-CD in the subarachnoid CSF: 3629.8 μg Eq/g in the subarachnoid space at the level of the high cervical spinal cord and 1054.4 μg Eq/g in the subarachnoid space at the level of the cerebral cortex. The fourth ventricle and the lateral cerebral ventricle had a concentration of 3173.9 and 1615 μg Eq/g, respectively. The cerebellum and cervical spinal cord, both immediately adjacent to the CBMC, had the highest concentrations of 275.1 and 302.5 μg Eq/g, respectively (Table 1). Similarly, CSF-adjacent regions of the cerebral cortex of the ventral frontal lobe (107.4 μg Eq/g), the cerebral cortex of the ventral temporal lobe (187.9 μg Eq/g), the ventral midbrain (229.5 μg Eq/g), and the ventral medulla (167.9 μg Eq/g) all had high concentrations of [^{14}C]-HP-β-CD. Interestingly, lower concentrations were found in the dorsal portions of these areas (cerebral cortex of the dorsal frontal lobe, 1.2 μg Eq/g; cerebral cortex of the dorsal temporal lobe, 3.6 μg Eq/g; dorsal midbrain, 1.2 μg Eq/g; and dorsal medulla, 28.1 μg Eq/g). The concentration observed in nasal turbinates remained relatively high at 528.1 μg Eq/g at 1 hour postdose.

At 4 hours postdose, the frontal and temporal lobes reached their highest concentrations, as did the midbrain. The finding at 1 hour postdose of higher concentration in ventral portions of the brain is not as evident at 4 hours, with higher dorsal concentrations now found in the cerebral cortex of the frontal lobe (204.6 μg Eq/g), the cerebral cortex of the parietal lobe (188.4 μg Eq/g), and the dorsal midbrain (166.1 μg Eq/g) (Table 1). At 4 hours postdose, the concentration observed in the nasal turbinates declined more than 2-fold, but remained relatively high at 223.7 μg Eq/g.

Levels began to steadily decline in the CNS at the 8-, 12-, and 24-hour time points (Table 1). Most tissues were at their lowest concentration by 24 hours postdose, although some tissue concentrations peaked or troughed

for a second time. Concentrations in the dorsal cerebellum rose between 4 and 8 hours postdose, before declining again, and between the 8 and 12 hours postdose, the concentration increased in the lateral ventricles, temporal lobe, ventral midbrain, ventral medulla, and ventral cervical spinal cord before decreasing again at the 24-hour mark. Between 12 and 24 hours postdose, the concentrations continued to decline in the frontal and temporal lobes, midbrain, cerebellum, cervical spinal cord, and subarachnoid space, however, those in the blood and fourth ventricle rose again. In the nasal turbinates, concentrations increased slightly between 8 and 12 hours postdose before declining at the final 24-hour mark. Concentrations at 24 hours postdose in CNS tissues ranged from 7.2 μg Eq/g in dorsal spinal cord to 44.1 μg Eq/g in the cerebrum. Concentrations in other extraneural tissue are present in Supplemental Table S1.

3.1 | Brain tissue pharmacokinetic data reveal moderately prolonged elimination times for [^{14}C]-HP-β-CD after CBMC administration in normal cats

The maximal observed tissue concentration (C_{max}) after a CBMC injection was observed 1 hour postdose for most tissues examined, and were highest in the cervical spinal cord, medulla, midbrain, and cerebellum; all areas closest to the injection site (Table 2). Tissue half-life ($t_{1/2}$) values were determined for specific regions of the brain and spinal cord and ranged from 7.6 hours in the ventral cerebellum to 105.1 hours in the dorsal medulla. Most $t_{1/2}$ values for brain regions ranged from about 11 to 16 hours. Tissue radioactivity C_{max} value for nasal turbinates was 1031.5 μg Eq/g at 0.25 hours postdose, with a $t_{1/2}$ of 17.6 hours (Table 2). Mean pharmacokinetic parameters of radioactivity in extraneural tissues are shown in Supplemental Table S2.

TABLE 2 Pharmacokinetic parameters of total radioactivity from brain tissue of normal cats after a single 120-mg intrathecal injection of [^{14}C]-HP-β-CD at the CBMC

	Pharmacokinetic parameters of brain tissue						
Tissue	T_{max} (h)	C_{max} (μg Eq/g)	AUC_{last} (μg Eq h/g)	AUC_{inf} (μg Eq h/g)	$t_{1/2}$ (h)	r^2	# pts in $t_{1/2}$
Blood (cardiac)	1	40.0	140.2	159.9	ND	0.2	4
Nasal turbinates	0.25	1031.5	3163.1	3952.1	17.6	0.9	3
Dorsal cerebral cortex,frontal lobe	4	204.6	1863.3	2747.4	15.1	1.0	3
Ventral cerebral cortex, frontal lobe	4	188.0	1965.3	2811.5	14.5	0.9	3
Dorsal cerebral cortex,at pituitary gland	4	188.4	1876.6	2900.9	16.1	1.0	3
Ventral cerebral cortex,at pituitary gland	1	187.9	1139.0	1404.2	9.9	1.0	2
Dorsal midbrain	4	166.1	1384.6	1612.0	7.9	0.8[a]	3
Ventral midbrain	1	229.5	1969.3	2167.4	17.9	0.6[a]	3
Dorsal cerebellum,at the fourth ventricle	1	275.1	1519.7	2043.1	13.4	0.72[a]	4
Ventral cerebellum,at the fourth ventricle	1	263.9	1969.3	2167.4	7.6	0.9	3
Dorsal medulla	1	28.1	441.5	3312.9	105.1	1.0	3
Ventral medulla	1	167.9	1254.9	1473.9	12.0	0.9	3
Dorsal cervical spinal cord	1	302.5	1448.1	1528.5	7.7	1.0	3
Ventral cervical spinal cord	0.25	278.4	1334.4	1603.9	15.7	0.5[a]	3
fourth ventricle	0.25	4026.6	8656.4	9002.7	10.7	1.0	3
Lateral cerebral ventricle	1	1615.0	3845.7	4104.6	10.5	0.8[a]	4
Subarachnoid space(high cervical spinal cord)	4	4196.7	9935.7	11 472.6	29.1	1.0	3
Subarachnoid space(cerebral cortex)	0.25	1726.5	10 660.1	12 118.3	11.9	1.0	4

Abbreviations: AUC, area under the tissue concentration-time curve; AUC_{inf}, AUC from time 0 to infinity with extrapolation of the terminal phase; AUC_{last}, AUC from time 0 to the time corresponding to the last quantifiable tissue concentration; C_{max}, maximal observed tissue concentration; CBMC, cerebromedullary cistern; HP-β-CD, 2-hydroxypropyl-β-cyclodextrin; ND, not determined; $t_{1/2}$, half-life; T_{max}, time correspondent to the maximum observed tissue concentration.

[a]$t_{1/2}$ is considered to be reliable if $r^2 \geq 0.85$ and there are >2 points used for $t_{1/2}$; $t_{1/2}$ value falls outside those criteria and should be considered with caution, as only an estimate.

TABLE 3 Concentrations (μg Eq/g) of radioactivity in tissues of normal cats after a single 120-mg intrathecal injection of [^{14}C]-HP-β-CD at the CBMC

		μg Eq/g tissue (mM)					
Tissue		**0.25 h**	**1 h**	**4 h**	**8 h**	**12 h**	**24 h**
Cerebrum	hi	NA	302.1 (0.21)	417.9 (0.29)	78.9 (0.05)	60.3 (0.04)	53.3 (0.04)
	med	NA	119.6 (0.08)	147.9 (0.10)	NM	NM	NM
	low	8.4 (0.01)	BQL	11.2 (0.01)	4.39 (0.003)	25.7 (0.02)	13.6 (0.01)
Cerebellum	hi	NA	689.5 (0.48)	403.0 (0.28)	44.3 (0.03)	44.4 (0.03)	49.7 (0.03)
	med	NA	277.6 (0.19)	149.3 (0.10)	NM	NM	NM
	low	19.3 (0.01)	7.9 (0.01)	11.0 (0.01)	11.84 (0.01)	19.9 (0.01)	22.48 (0.02)

Note: The lower limit of quantification was determined by using the radioactive concentration (μCi/g) of the lowest calibration standard used to generate a calibration curve divided by the specific activity of the test article (1.76 μCi/mg).
Abbreviations: BQL, below quantification limit; CBMC, cerebromedullary cistern; CNS, central nervous system; hi, highest concentration; HP-β-CD, 2-hydroxypropyl-β-cyclodextrin; lo, lowest concentration; med, median concentration; NA, not available; NM, not measured.

TABLE 4 Summary of total radioactivity reveals varying tissue concentration gradients within specific regions of the CNS in normal cats after a single 120-mg intrathecal injection of [^{14}C]-HP-β-CD at the CBMC

	CNS tissue concentration gradients					
CNS Region	Concentration μg Eq/g (mM)	Location	Concentration μg Eq/g (mM)	Location	Concentration μg Eq/g (mM)	Location
	8 h		12 h		24 h	
Frontal lobe	93.8 (0.07)	Dorsal cortex	96.7 (0.07)	Dorsal cortex	74.0 (0.05)	Dorsal cortex
Max						
Min	51.7 (0.04)	Core	59.0 (0.04)	Core	43.9 (0.03)	Core
Temporal lobe	100.6 (0.07)	Ventral cortex	77.0 (0.05)	Ventral cortex	73.9 (0.05)	Ventral cortex
Max						
Min	2.6 (0.002)	Core	25.8 (0.02)	Core	5.6 (0.004)	Core
Midbrain	76.1 (0.05)	Surface	58.9 (0.04)	Surface	49.0 (0.03)	Surface
Max						
Min	26.3 (0.02)	Core	29.1 (0.02)	Core	8.7 (0.006)	Core
Cerebellum	57.2 (0.04)	Cortex	73.1 (0.05)	Cortex	81.5 (0.06)	Cortex
Max						
Min	7.3 (0.01)	White matter	11.5 (0.01)	White matter	6.0 (0.004)	White matter
Medulla	32.8 (0.02)	Surface	64.6 (0.04)	Surface	17.2 (0.01)	Surface
Max						
Min	13.7 (0.01)	Core	8.4 (0.01)	Core	10.2 (0.007)	Core
Spinal cord	91.4 (0.06)	Surface	67.6 (0.05)	Surface	79.3 (0.06)	Surface
Max						
Min	15.5 (0.01)	Core	46.0 (0.03)	Core	16.0 (0.01)	Core

Note: LLOQ = 0.0003372 μCi/g/0.00164 μCi/μg = 0.206 μg Eq/g tissue ULOQ = 5.3824631 μCi/g/0.00164 μCi/μg = 3280.990 μg Eq/g tissue.
Abbreviations: CBMC, cerebromedullary cistern; CNS, central nervous system; HP-β-CD, 2-hydroxypropyl-β-cyclodextrin LLOQ, lower limit of quantification; max, maximum; min, minimum; ULOQ, upper limit of quantitation.

The area under the tissue concentration-time curve from time 0 to infinity with extrapolation of the terminal phase (AUC_{inf}) determined for specific brain regions ranged from 1404.2 μg Eq h/g in the temporal lobe cortex to 3312.9 μg Eq h/g for the dorsal medulla (Table 2). The area under the tissue concentration-time curve from time

0 to the time correspondent to the last quantifiable concentration (AUC_{last}) determined for specific brain regions ranged from 441.5 μg Eq h/g in the dorsal medulla to 1969.3 μg Eq h/g for the ventral cerebellum. Although the $t_{1/2}$ of the dorsal medulla appeared reliable, due to the conformance to acceptance criteria, the large difference between AUC_{last} and AUC_{inf} suggested that the $t_{1/2}$ value did not accurately portray the actual elimination rate and may have reflected continued distribution throughout the organ, and/or a levelling of the peak concentration. The highest AUC values of [^{14}C]-HP-β-CD were observed in the ventricles and subarachnoid spaces surrounding the brain and spinal cord. Cerebrospinal fluid-filled regions of the CNS had AUC_{inf} values ranging from 4104.6 μg Eq h/g for lateral cerebral ventricle to 12 118.3 μg Eq h/g for the CSF surrounding the high cervical spinal cord, while AUC_{last} values ranged from 3845.7 μg Eq h/g for lateral cerebral ventricle to 10 660.1 μg Eq h/g for CSF surrounding high cervical spinal cord. The $t_{1/2}$ values in ventricles and subarachnoid spaces surrounding the brain and spinal cord ranged from about 11 to 30 hours (Table 2).

3.2 | HP-β-CD penetrates brain parenchyma in a gradient pattern and does not reduce cholesterol storage in subcortical nuclei of CBMC-treated affected NPC1 cats

Due to the visible parenchymal concentration gradient observed at 4 hours postdose (Supplemental Figure S3), different areas within the temporal lobe and cerebellum were sampled and identified as "hi" (dark grey region adjacent to subarachnoid space), "med" (mod-light grey region), and "lo" (light grey to white region farthest from subarachnoid space) in an attempt to show the range of concentrations observed in the same tissue relative to

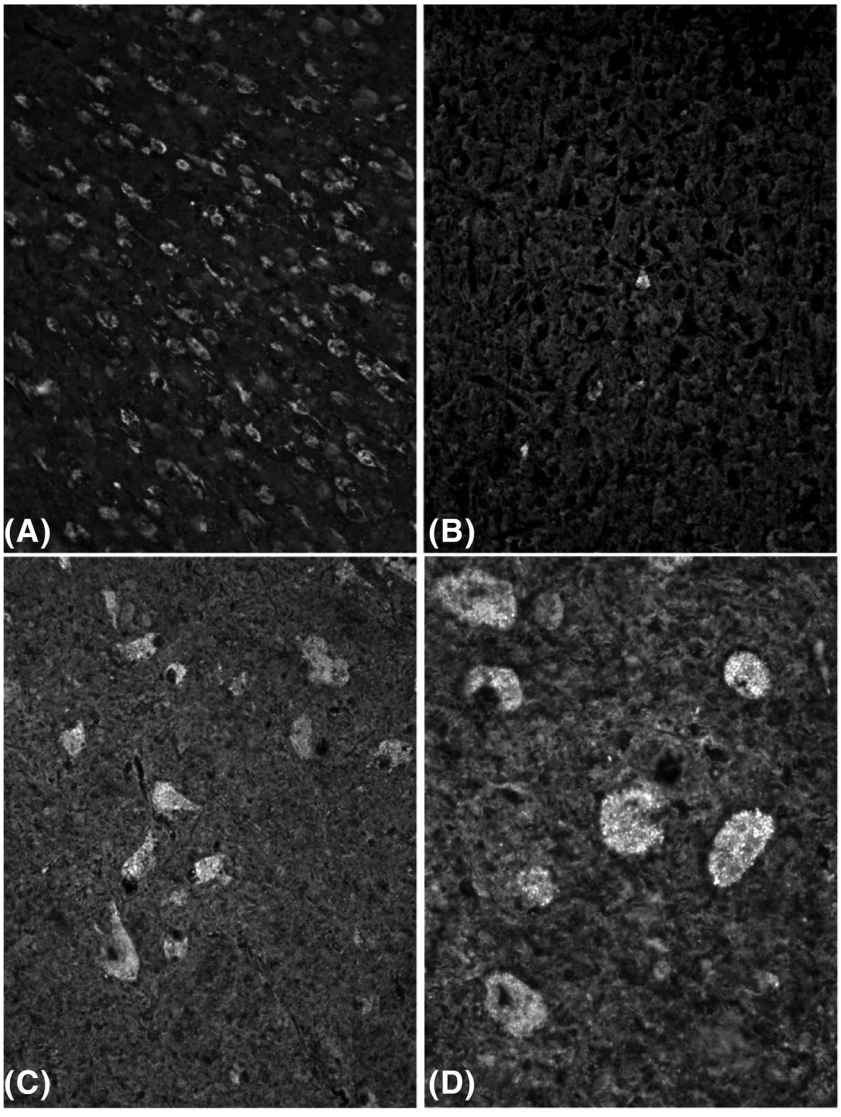

FIGURE 4 Persistent cholesterol storage as assessed by filipin staining in neurons of untreated NPC1 cats (A, C) and in NPC1 cats that received 120-mg intrathecal injections of [^{14}C]-HP-β-CD at the CBMC (B, D). A, B, cerebral cortex; C, thalamic nucleus; D, deep cerebellar nuclei. CBMC, cerebellomedullary cistern; HP-β-CD, 2-hydroxypropyl-β-cyclodextrin; NPC1, Niemann-Pick Type C

their proximity to the subarachnoid space (Table 3). At 4 hours postdose, the cerebrum reached a C_{max} of 417.9 μg Eq/g, and the highest concentration in the cerebellum cortex was 403.0 μg Eq/g (Table 3; Supplemental Figure S3). In regions of these two tissues farthest from the subarachnoid space, the concentration in the cerebrum and cerebellum measured 11.2 and 11.0 μg Eq/g, respectively, and only increased to maximum values of 25.7 and 22.48 μg Eq/g, respectively.

Further image analysis was conducted on brain images collected from cats at 8, 12, and 24 hours postdose to determine the penetration of HP-β-CD into the frontal and temporal lobes, midbrain, cerebellum, medulla, and spinal cord (Table 4). Concentration data were collected at continuous intervals of 100 μm over an area that was 1 mm wide, spanning the entire region of each brain location previously listed. These data (Table 4) show that there were large differences measured in the concentrations of [^{14}C]-HP-β-CD going from the surface of the brain and spinal cord nearest the subarachnoid space, to the inner depths of those regions which were farthest from the subarachnoid space. At 8 hours postdose there was an approximate 2-fold difference in the concentrations between surface to inner regions of the medulla and frontal lobe, an approximate 3-fold difference in the concentrations between surface to inner midbrain, an approximate 8-fold difference in the concentrations between surface to inner cerebellum, and an approximate 50-fold difference in the concentrations between surface to inner temporal lobe. The differences in most regions increased over time, except for the frontal lobe and medulla. At 24 hours postdose there was approximately a 13- to 14-fold difference in

TABLE 5 Comparison of CNS tissue concentrations following after a single 120-mg intrathecal injection of [^{14}C]-HP-β-CD at the CBMC or LC

	CNS tissue concentrations (μg Eq/g tissue)			
	CBMC		LC	
Tissue	8 h	12 h	8 h	12 h
Blood (cardiac)	0.8 (<0.01)	0.4 (<0.01)	2.5 (<0.01)	2.4 (<0.01)
Brain (entire)	NS	NS	3.3 (<0.01)	9.9 (0.01)
Cerebrum hi	79.0 (0.05)	60.3 (0.04)	4.7 (<0.01)	14.2 (0.01)
low	4.4 (<0.01)	25.8 (0.02)	1.3 (<0.01)	2.5 (<0.01)
Medulla cerebellum	20.5 (0.01)	41.6 (0.03)	2.9 (<0.01)	7.2 (0.01)
hi	44.3 (0.03)	44.4 (0.03)	9.5 (0.01)	13.3 (0.01)
low	11.8 (0.01)	20.0 (0.01)	1.7 (<0.01)	2.9 (<0.01)
Spinal cord	36.3 (0.03)	54.7 (0.04)	24.9 (0.02)	41.9 (0.03)

Abbreviations: CBMC, cerebromedullary cistern; CNS, central nervous system; HP-β-CD, 2-hydroxypropyl-β-cyclodextrin; hi, highest concentration; LC, lumbar cistern; low, lowest concentration; NS, no sample.

TABLE 6 Comparison of CNS tissue concentrations following after a single 120-mg intrathecal injection of [^{14}C]-HP-β-CD at the CBMC or LC

		CNS tissue concentrations (μg Eq/g tissue)			
		CBMC		LC	
Tissue		8 h	12 h	8 h	12 h
Blood (cardiac)		0.8 (<0.01)	0.4 (<0.01)	2.5 (<0.01)	2.4 (<0.01)
Brain (entire)		NS	NS	3.3 (<0.01)	9.9 (0.01)
Cerebrum	hi	79.0 (0.05)	60.3 (0.04)	4.7 (<0.01)	14.2 (0.01)
	low	4.4 (<0.01)	25.8 (0.02)	1.3 (<0.01)	2.5 (<0.01)
Medulla		20.5 (0.01)	41.6 (0.03)	2.9 (<0.01)	7.2 (0.01)
Cerebellum	hi	44.3 (0.03)	44.4 (0.03)	9.5 (0.01)	13.3 (0.01)
	low	11.8 (0.01)	20.0 (0.01)	1.7 (<0.01)	2.9 (<0.01)
Spinal cord		36.3 (0.03)	54.7 (0.04)	24.9 (0.02)	41.9 (0.03)

Abbreviations: CBMC, cerebromedullary cistern; CNS, central nervous system; HP-β-CD, 2-hydroxypropyl-β-cyclodextrin; hi, highest concentration; LC, lumbar cistern; low, lowest concentration; NS, no sample.

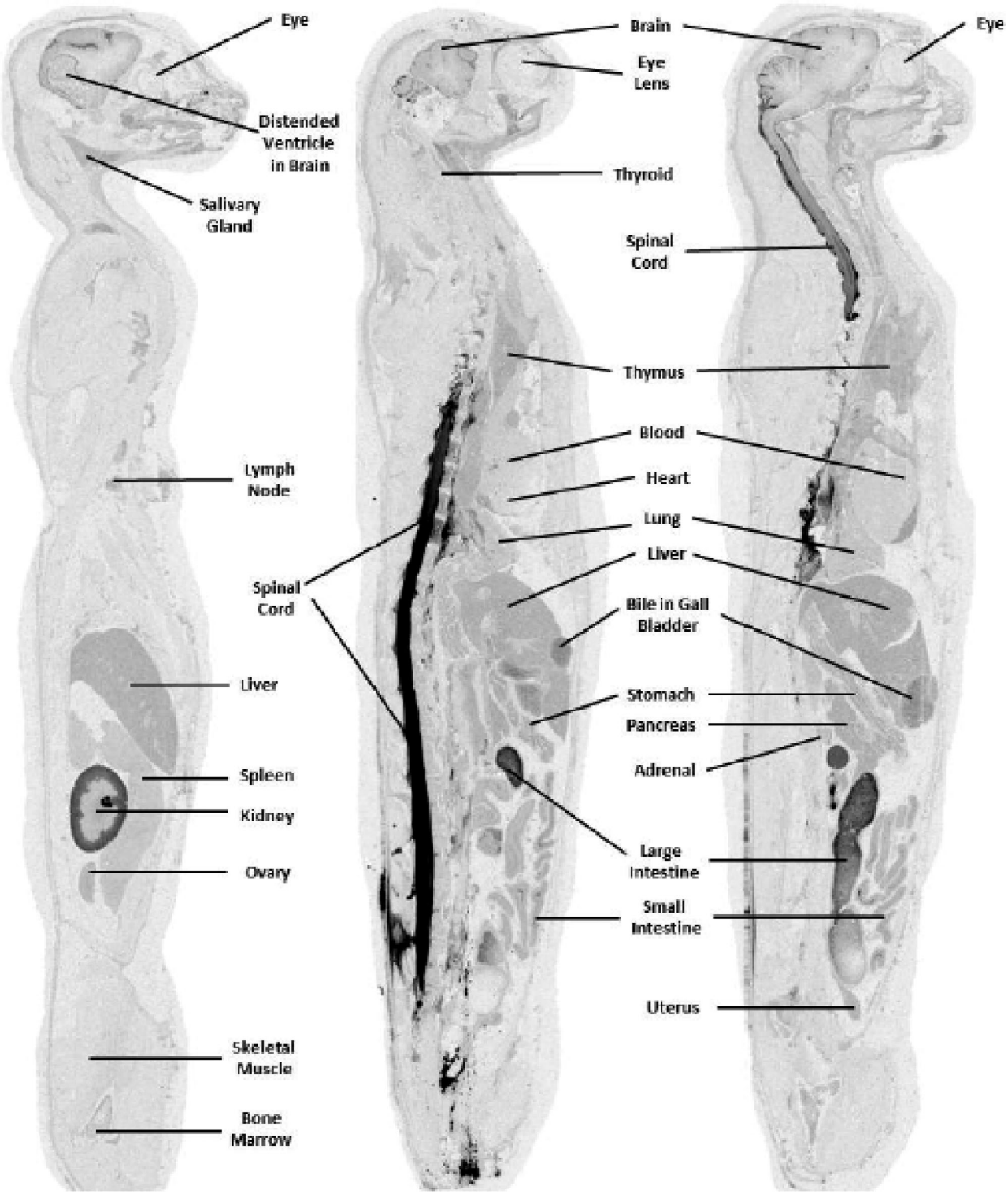

FIGURE 5 Whole-body autoradiogram of radioactivity distribution in a normal cat 8 hours postdose, following a single intrathecal injection of [^{14}C]-HP-β-CD at the lower LC. Sections are parasagittal and sagittal. HP-β-CD, 2-hydroxypropyl-β-cyclodextrin; LC, lumbar cistern

the concentrations between surface to inner regions of the temporal lobe and cerebellum, respectively, and a 5-fold difference between surface to inner regions of the midbrain. Similar differences were observed in spinal cord.

The NPC1 cats were injected with 120 mg HP-β-CD every 2 weeks for life via the CBMC beginning at 3 weeks of age. Recently, tissues from three 24-week-old cats from the study were analysed for storage material and

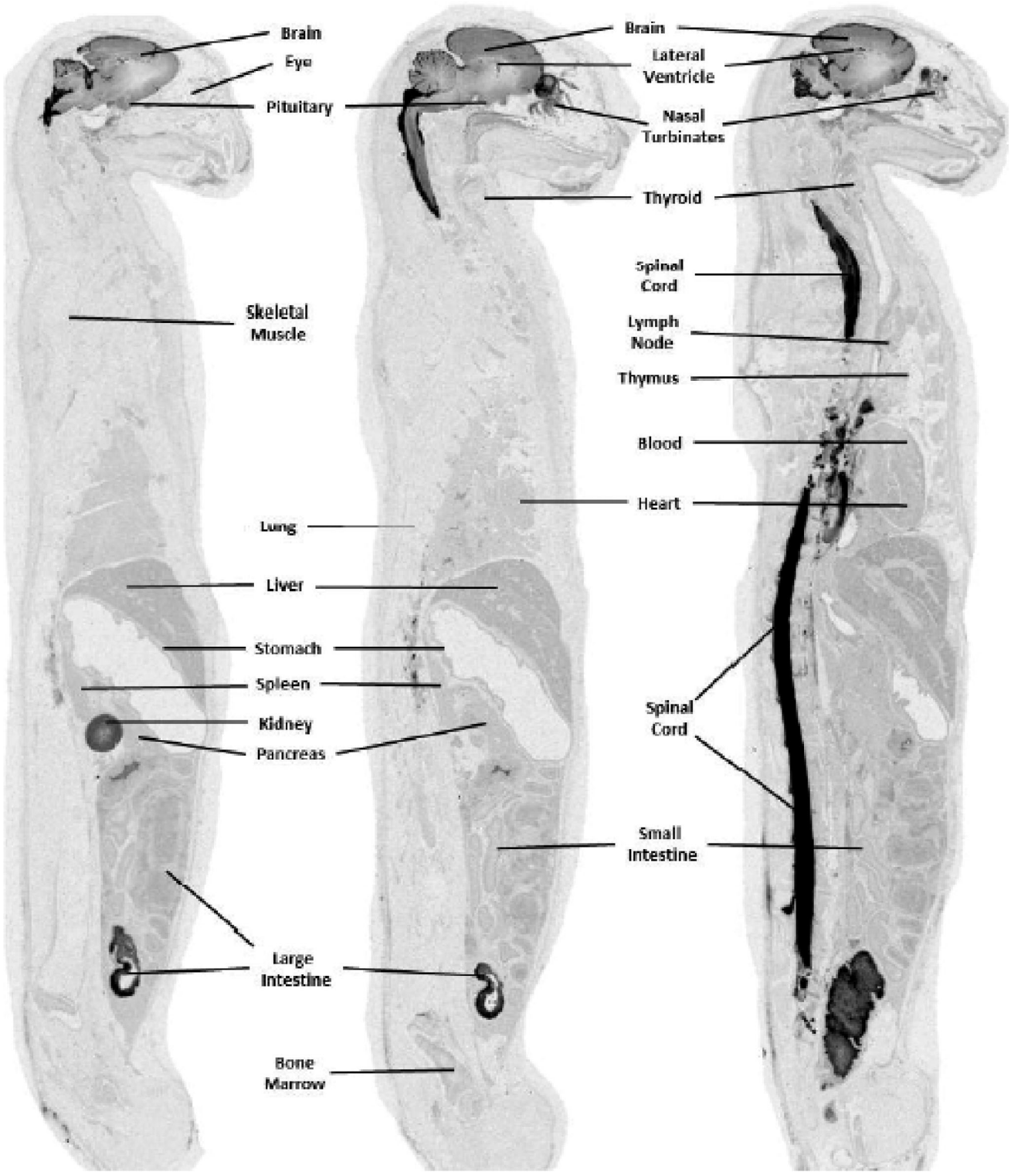

FIGURE 6 Whole-body autoradiogram of radioactivity distribution in a normal cat 12 hours postdose, following a single intrathecal injection of [^{14}C]-HP-β-CD at the lower LC. Sections are parasagittal and sagittal. HP-β-CD, 2-hydroxypropyl-β-cyclodextrin; LC, lumbar cistern

compared to untreated NPC1 cats. Interestingly, while the cerebral and cerebellar cortices showed significant clearage of storage (Figure 4A, B), deep brain nuclei, including the thalamic nuclei and deep cerebellar nuclei, continued to show significant neuronal swelling and storage (Figure 4C, D). In the present study, these regions of the brain correspond to regions of lowest exposure to [^{14}C]-HP-β-CD.

TABLE 7 Comparison of CNS tissue concentrations following after a single 120-mg intrathecal injection of [^{14}C]-HP-β-CD at the CBMC or LC

		CNS tissue concentrations (μg Eq/g tissue)			
		CBMC		LC	
Tissue		8 h	12 h	8 h	12 h
Blood (cardiac)		0.8	0.4	2.5	2.4
Brain (entire)		NS	NS	3.3	9.9
Cerebrum	hi	79.0	60.3	4.7	14.2
	low	4.4	25.8	1.3	2.5
Medulla		20.5	41.6	2.9	7.2
Cerebellum	hi	44.3	44.4	9.5	13.3
	low	11.8	20.0	1.7	2.9
Spinal cord		36.3	54.7	24.9	41.9

Abbreviations: CBMC, cerebromedullary cistern; CNS, central nervous system; HP-β-CD, 2-hydroxypropyl-β-cyclodextrin; hi, highest concentration; LC, lumbar cistern; low, lowest concentration; NS, no sample.

TABLE 8 Tissue distribution of radioactivity in tissues of normal cats after a single 120-mg intrathecal injection of [^{14}C]-HP-β-CD at the CBMC or the LC

	[^{14}C]-HP-β-CD concentration (μg Eq/g tissue)							
	CBMC						LC	
Tissue	0.25 h	1 h	4 h	8 h	12 h	24 h	8 h	12 h
Blood	37.1	40.0	9.2	0.8	0.4	1.3	2.5	2.4
Bone marrow	1.7	4.4	1.7	0.3	0.4	0.9	3.8	2.4
Spleen	3.7	10.9	3.6	0.5	0.6	0.8	3.1	3.1
Kidney (cortex)	10.6	31.5	25.4	11.1	11.1	33.1	40.2	32.8
Liver	5.7	12.3	4.2	1.1	0.7	2.4	6.3	4.7
Bile (in gall bladder)	BQL	3.1	19.4	2.5	1.0	22.6	11.3	25.4
Urinary bladder (contents)	BQL	343.5	2842.8	412.4	542.6	295.6	4527.9	2833.8
Brain(cerebellum, high)	8.4	BQL	11.2	44.3	44.4	49.7	9.5	13.3
Brain (cerebrum, high)	NA	689.5	403.0	79.0	60.3	53.3	4.7	14.2
Brain (medulla)	12.5	36.6	116.4	20.5	41.6	12.2	2.9	7.2
Spinal cord	91.2	130.5	214.9	36.3	54.7	26.2	24.9	41.9
Nasal turbinates	1031.5	528.1	223.7	55.1	58.4	31.2	12.9	4.4
Large intestine (contents)	5.2	25.0	6.6	3.2	3.4	15.4	25.6	27.5
Small intestine (contents)	BQL	0.5	20.5	0.8	2.4	1.3	BQL	6.7
Stomach(gastric mucosa)	9.8	16.4	4.4	1.1	0.8	1.8	5.7	3.5

Abbreviations: BQL, below quantification limit; CBMC, cerebromedullary cistern; HP-β-CD, 2-Hydroxypropyl-β-cyclodextrin; LC, lumbar cistern; NA, not assessed.

3.3 | Tissue concentration and distribution of [^{14}C]-HP-β-CD after lower lumbar injections indicates reduced brain penetration compared to CBMC administration

Two cats, 1 male and 1 female, were injected with [^{14}C]-HP-β-CD via the lower LC and data were collected at 8 and 12 hours postdose. Overall QWBA data indicated that [^{14}C]-HP-β-CD was distributed from the lumbar region up to and surrounding the brain and was also widely distributed to peripheral tissues (Table 5 and Supplemental Table S3). A similar gradient of distribution was noted in the brain parenchyma as reported above for CBMC-injected cats (Figures 5 and 6). The concentration in blood was similar at 8 (2.5 μg Eq/g) and 12 hours

(2.4 μg Eq/g) postdose and was substantially higher than that observed in blood for animals given a CBMC injection (0.8 and 0.4 μg Eq/g at 8 and 12 hours, respectively). However, concentrations in the brain of cats at 8 and 12 hours after a lumbar injection (which ranged between 1.3 and 14.2 μg Eq/g) were substantially lower than that observed at similar times for cats given the CBMC injection (concentrations ranged between 4.4 and 79.0 μg Eq/g; Table 7). At 12 hours postdose, spinal cord concentrations were almost 3-fold higher than brain tissue following a lumbar delivery (41.9 vs 14.2 μg Eq/g for the cerebrum hi; Table 5). Spinal cord levels in CBMC treated cats were similar to brain levels at the 12-hour mark (54.7 vs 60.3 μg Eq/g for the cerebrum hi; Table 5). Concentrations in excretory tissues (ie, kidney and liver) of cats given a lumbar injection, however were higher than that observed in cats given a CBMC injection (range: 4.7 to 40.2 vs 0.7 to 11.1 μg Eq/g; Table 8). Comparison of CNS tissue concentrations 8 and 12 hours after CMBC and LC injection indicated higher [^{14}C]-HP-β-CD concentrations were observed following the 120-mg CMBC injection (Table 5).

4 | DISCUSSION

This study identified the distribution and tissue penetration of [^{14}C]-HP-β-CD to the CNS of normal cats via IT delivery. [^{14}C]-HP-β-CD-derived radioactivity was absorbed from the CBMC and was widely distributed to tissues of the cats after a single IT dose of [^{14}C]-HP-β-CD. Most CNS tissues (8 of 18) were observed to have reached their highest concentration at 1 hour postdose. The highest concentration in blood was 40.0 μg Eq/g, which occurred at 1 hour postdose, and decreased to 9.2 μg Eq/g at 4 hours.

The low but detectable blood concentration at 24 hours was most likely due to a continued slow distribution of [^{14}C]-HP-β-CD-derived radioactivity from the CNS into the vasculature. Visual examination of the autoradiographs showed that, while concentrations in most tissues were decreasing, penetration of [^{14}C]-HP-β-CD-derived radioactivity into the deeper parts of the CNS tissues was ongoing and concentrations were highest at the last time point of 4 hours postdose. We previously showed that a $t_{1/2}$ of 0.7-2.6 hours was achieved following IT administration of 120 mg of HP-β-CD at the CBMC of normal cats (Vite et al 2015). The total CSF volume in the cat is approximately 4.5 mL and CSF is produced at a rate of 20-22 μL/minute with an estimated turnover time of 3 hours (Davson et al 1962; Davson and Segal, 1995) which approximates the experimental half-life. However, in the present study, the $t_{1/2}$ in brain parenchyma was over 5-fold greater than that found in the CSF suggesting that HP-β-CD is being retained in cells and/or the extracellular matrix. HP-β-CD does not cross cell membranes due to its size and polarity. Therefore, its mechanism of action is through fluid-phase pinocytosis and delivery to the late endosomal and lysosomal compartments where it facilitates cholesterol release from the lysosome without the need for NPC1 or NPC2 function (Rosenbaum et al 2010). This explains the finding of its continued effects on cholesterol reduction in cultured cells after cyclodextrin has been removed from the media (Rosenbaum et al 2010). Additionally, cyclodextrins are proposed to bind to the glycocalyx of the brain vasculature (Pontikis et al 2013; Banks et al 2019). It is possible that binding of HP-β-CD to the extracellular matrix would similarly increase its half-life in brain parenchyma. The cellular and extracellular distribution of radioactive HP-β-CD was not evaluated in this study; however, electron microscopy would provide an answer to the location of cyclodextrin within the parenchyma.

Tissues, besides the CNS, with the highest concentrations (≥100 μg Eq/g) of radioactivity were nasal turbinates (1031.5 μg Eq/g or 0.7 μM at 0.25 hours postdose) and pituitary gland (426.4 μg Eq/g or 0.3 μM at 0.25 hours postdose). High concentrations were also present in the contents of the urinary bladder (2842.8 μg Eq/g or 2.0 μM at 4 hours postdose), which demonstrated that renal excretion was the major route of elimination during the first 4 hours postdose. This finding has been previously reported in pharmacokinetics studies of lipophiles in mice.[9] Prolonged exposure of tissues that are outside of the CNS is expected, albeit at low concentrations, as [^{14}C]-HP-β-CD-derived radioactivity is eliminated from the CNS compartment and then eliminated from the body. Interestingly, the highest tissue concentration was observed in the nasal turbinates at 0.25 hours postdose, which suggested that [^{14}C]-HP-β-CD-derived radioactivity was rapidly transported out of the CNS into the general circulation via the olfactory nerves and nasal turbinates. These same pathways, in reverse, have been exploited in delivery of therapeutics to the brain via intranasal injections.[10]

A possible explanation for the lower brain penetration after an LC injection as compared to that achieved by the CBMC injection was the proximity of the dose site to the brain. In the case of the LC injection, a higher amount of radioactivity probably distributed out from the injection site (ie, along and through vertebral spaces and/or peripheral nerves of the lumbar region), into surrounding tissues and vasculature, and was subsequently eliminated through renal and biliary excretion before reaching the brain. Radioactivity injected into the CBMC had a much higher chance of distributing into the brain before being distributed into the surrounding tissues and vasculature and subsequently eliminated from the body. This theory is supported by the observation of higher concentrations

in the urine and bile of cats given the lumbar injections (urine: 4528 μg Eq/g at 8 hours and 2834 μg Eq/g at 12 hours; bile: 11.3 μg Eq/g at 8 hours and 25.4 μg Eq/g at 12 hours) than in those given a CBMC injection (412 μg Eq/g at 8 hours and 543 μg Eq/g at 12 hours; bile: 2.5 μg Eq/g at 8 hours and 1.0 μg Eq/g at 12 hours) (Table 8).

A concentration gradient was identified in CNS tissue regardless of the injection site. Quantitative analysis of brain tissue from frontal cortex to spinal cord revealed that [^{14}C]-HP-β-CD concentrations were highest in the outermost region and lowest at the innermost region of the tissues examined. Filipin staining in frontal cortex sections from 120 mg-treated-NPC1 cats identified a dramatic reduction of cholesterol storage in cortical neurons (Figure 4A, B). However, deeper structures, like the thalamus were found to still harbour abnormal cholesterol storage (Figure 4C, D). The lowest concentrations at the latest time point (24 hours postdose) in the inner most regions of these structures were quantified at 43.9 or 0.03 μM and 6.0 μg Eq/g, or 0.004 μM, respectively. It is evident that higher HP-β-CD concentrations are needed for longer periods of time at deeper structures such as the thalamus. Previous in vitro studies have identified that HP-β-CD concentrations as low as 0.1 mM effectively released cholesterol in late endosomes and lysosomes of neurons and glial cells while simultaneously increasing cholesterol at the endoplasmic reticulum (ER), whereas 1 mM HP-β-CD concentrations removed cholesterol from the plasma membrane and ER.[11] From these studies, a 10-fold higher concentration is necessary to completely clear aberrant cholesterol storage in cells. This appears to be a similar in vivo finding in treated cat brain tissue considering that the lowest concentration of the inner most frontal cortex is ~10-fold higher than the lowest inner most concentrations of the cerebellum (0.03 vs 0.004 μM, respectively) where a discrepancy in cholesterol storage exists.

The phase 3 portion of the clinical trial evaluating the administration of HP-β-CD at the lumbar IT space in NPC1 patients is now completed and data is being evaluated. In the published phase 2 trial, 600-1200 mg of HP-β-CD were injected intrathecally monthly in NPC1 patients (Ory et al 2017). Human patients received approximately 900 mg per 1300 g brain weight and 150 mL CSF volume providing a calculation of 0.7 mg/g brain weight and 6 mg/mL CSF. In contrast, in this study cats received 120 mg cyclodextrin per 30 g brain weight and 4.5 mL CSF volume providing a calculation of 4 mg/g brain weight and 27 mg/mL CSF. Therefore, cats received approximately a 6-fold higher dose as calculated by brain weight and 4.5-fold higher dose as calculated by CSF volume. Finally, the diameter of the cat brain is approximately 4 cm and of the human brain approximately 14 cm. Taken together, the concentration of HP-β-CD in the deep brain of human patients is predicted to be very low and likely insufficient to influence pathology. However, if we assume that lumbar IT administration, as done in patients, results in even a 4-fold decrease in brain concentration, the dose patients are receiving is similar to the dose of 7.5 mg HP-β-CD which still resulted in substantial improvement in cerebellar ataxia and in reduction of cerebral and cerebellar cortical cholesterol storage (Vite et al 2015).

Based on the findings in the study, one might suggest that the dose of HP-β-CD could be increased in NPC1 patients. However, HP-β-CD also results in ototoxicity which, predictably, was severe in cats receiving 120 mg and more modest in children receiving 600 mg. Therefore, ototoxicity is likely to be a dose-limiting factor in patients (Vite et al 2015; Ory et al 2017). It is hypothesised that intracerebroventricular administration could further increase brain concentration and may also treat deeper brain regions. This method of administration has not been evaluated in cats.

Finally, the data presented above assumes that brain weight and CSF volume is similar in normal cats and NPC1 cats. Although the brain weight of normal cats is predictably 30 mg, NPC1 cats have a lower brain weight of approximately 25 mg at end stage disease (approximately 24 weeks of age) (unpublished data). Similarly, NPC1 cats have a lower body weight at 6 months of age compared to normal control cats (Vite et al 2008). Therefore, it is likely that the doses reported in the normal cats above would be higher in NPC1 cats.

The data presented above suggest that the improvement in cerebellar ataxia, and the improvement in cerebrocortical and cerebellocortical storage, is associated with high concentrations of HP-β-CD in these regions and that deeper brain regions accumulate lower concentrations of HP-β-CD. It we assume that resolution of neuronal storage is dependent on HP-β-CD concentration, we predict that storage in the basal ganglia, cerebellar nuclei, and brainstem would not be as effectively treated. A study to evaluate the histopathology throughout the NPC1 cat brain is currently in progress.

ACKNOWLEDGEMENTS

We thank Holly Adams for her excellent technical writing support.

This work was partially supported by the following grants: NIH R01-NS073661, P40-02512, Ara Parseghian Medical Research Foundation, Dana's Angels Research Trust, Race for Adam, National Niemann-Pick Disease Foundation, Support of Accelerated Research for Niemann-Pick Type C Disease, R01 NS081985, P30

DK020579, the German Research Foundation (DFG-STE 1069/2-1), R01-HD045561, and R01 NS053677.

CONFLICT OF INTEREST

Three authors are employed by pharmaceutical or assay.

Laboratories but have no competing interests: Janssen Research & Development (M.L.K., S.S.), Madrigal Pharmaceuticals (E.S.), XenoBiotic Laboratories, Inc. (A.L.).

AUTHOR CONTRIBUTIONS

Each author made substantial contributions to the design of the work and the acquisition, analysis, and interpretation of data. Each author reviewed and revised the manuscript and gave final approval. Each author agrees to be accountable for all aspects of the work.

ORCID

Charles H. Vite https://orcid.org/0000-0001-6625-5266

REFERENCES

1. Gould S, Scott R. 2-Hydroxypropyl-beta-cyclodextrin (HP-beta-CD): a toxicology review. *Food Chem Toxicol*. 2005;43:1451-1459.
2. Brewster ME, Anderson WR, Meinsma D, et al. Intravenous and oral pharmacokinetic evaluation of a 2-hydroxypropyl-beta-cyclodextrin-based formulation of carbamazepine in the dog: comparison with commercially available tablets and suspensions. *J Pharm Sci*. 1997;86:335-339.
3. Vanier MT. Niemann-Pick disease type C. *Orphanet J Rare Dis*. 2010;5:16.
4. Camargo F, Erickson RP, Garver WS, et al. Cyclodextrins in the treatment of a mouse model of Niemann-Pick C disease. *Life Sci*. 2001;70:131-142.
5. Liu B, Turley SD, Burns DK, Miller AM, Repa JJ, Dietschy JM. Reversal of defective lysosomal transport in NPC disease ameliorates liver dysfunction and neurodegeneration in *npc*1−/− mouse. *Proc Natl Acad Sci U S A*. 2009;106:2377-2382.
6. Davidson CD, Ali NF, Micsenyi MC, et al. Chronic cyclodextrin treatment of murine Niemann-Pick C disease ameliorates neuronal cholesterol and glycosphingolipid storage and disease progression. *PLoS One*. 2009;4:e6951. https://doi.org/10.1371/journal.pone.0006951.
7. Vite, C. H., J. H. Bagel, G. P. Swain, M. Prociuk, T. U. Sikora, V. M. Stein, P. O'Donnell, T. Ruane, S. Ward, A. Crooks, S. Li, E. Mauldin, S. Stellar, M. De Meulder, M. L. Kao, D. S. Ory, C. Davidson, M. T. Vanier, and S. U. Walkley. 2015. Intracisternal cyclodextrin prevents cerebellar dysfunction and Purkinje cell death in feline Niemann-Pick type C1 disease. *Sci Transl Med* 7: 276ra26. doi: https://doi.org/10.1126/scitranslmed.3010101
8. Ory DS, Ottinger EA, Farhat NY, et al. Intrathecal 2-hydroxypropyl-β-cyclodextrin decreases neurological disease progression in Niemann-Pick disease, type C1: a non-randomized, open-label, phase 1-2 trial. *Lancet*. 2017;390:1758-1768.
9. Pitha J, Gerloczy A, Olivi A. Parenteral hydroxypropyl cyclodextrins: intravenous and intracerebral administration of lipophiles. *J Pharm Sci*. 1994;83:833-837.
10. Dhuria SV, Hanson LR, Frey WH. Intranasal delivery to the central nervous system: mechanisms and experimental considerations. *J Pharm Sci*. 2010;99:1654-1673.
11. Peake KB, Vance JE. Normalization of cholesterol homeostasis by 2-hydroxypropyl-β-cyclodextrin in neurons and glia from Niemann-Pick C1 (NPC1)-deficient mice. *J Biol Chem*. 2012;287:9290-9298.

SUPPORTING INFORMATION

Additional supporting information may be found online in the Supporting Information section at the end of this article.

How to cite this article: Kao ML, Stellar S, Solon E, et al. Pharmacokinetics and distribution of 2-hydroxypropyl-β-cyclodextrin following a single intrathecal dose to cats. *J Inherit Metab Dis*. 2020;43:618–634. https://doi.org/10.1002/jimd.12189